



# Heat Transfer Performance of Uni-Directional and Bi-Directional Lid-Driven Cavities Using Nanoparticle Enhanced Ionic Liquids (NEILS)

Rajesh Nimmagadda<sup>1</sup> · Elena Ionela Chereches<sup>2</sup> · Marius Chereches<sup>2</sup>

Received: 13 January 2021 / Accepted: 8 February 2021 / Published online: 8 March 2021

© The Author(s), under exclusive licence to Springer Science+Business Media, LLC part of Springer Nature 2021

## Abstract

Two-dimensional numerical investigation has been carried out using an in-house CFD code to obtain the heat transfer performance of normal, uni-directional and bi-directional lid-driven cavity. The 2D in-house code is based on single phase approach for studying steady state laminar flows. Pure water (PW), ionic liquid (IL): 1-ethyl-3-methylimidazolium methanesulfonate;  $[C_2mim][CH_3SO_3]$ , ionic liquid mixtures (PW + IL) and alumina ( $Al_2O_3$ ) nanoparticle enhanced ionic liquids (NEILS) are used in the present investigation. The thermophysical properties of all the heat transfer fluids used in the present numerical investigation were obtained from the experimentally measured data available in the literature. The obtained results showed that uni-directional lid-driven cavity exhibits 68.78 % higher  $Nu_{avg}$  value at  $Re=1900$  in comparison with normal lid-driven cavity for pure water. The use of  $[C_2mim][CH_3SO_3]$  ionic liquid also enhances the heat transfer performance by exhibiting 115.48 % higher  $Nu_{avg}$  value in comparison with pure water at  $Re=1900$ . Moreover, 15 % wt  $Al_2O_3$  nanoparticles in 0.25PW + 0.75IL gives 21.2 % and 161.16 % higher heat transfer performance in comparison with ionic liquid and pure water respectively at  $Re=1900$ . Furthermore, it is also observed that 10 % wt  $Al_2O_3$  nanoparticles in 0.25PW + 0.75IL shows similar heat transfer performance like ionic liquid at all  $Re$ .

**Keywords** Bi-directional · Heat transfer · Ionic liquid · Nanoparticles · Uni-directional

---

This article is part of the Special Issue on Nanoparticle enhanced Ionic Liquids.

✉ Rajesh Nimmagadda  
rajesh.mech335@gmail.com

<sup>1</sup> Center for Advanced Energy Studies, Koneru Lakshmaiah Educational Foundation, Vaddeswaram, A.P., India

<sup>2</sup> Technical University “Gheorghe Asachi” of Iasi, Iasi, Romania

**Nomenclature**

$C_p$	Specific heat ( $\text{J}\cdot\text{kg}^{-1}\text{K}^{-1}$ )
$h$	Convective heat transfer coefficient ( $\text{W}\cdot\text{m}^{-1}\text{K}^{-1}$ )
$H$	Height (m)
$k$	Thermal conductivity ( $\text{W}\cdot\text{m}^{-1}\text{K}^{-1}$ )
$L$	Length (m)
$Nu$	Nusselt number
$p$	Pressure ( $\text{kg}\cdot\text{m}^{-1}\text{s}^{-2}$ )
$Pr$	Prandtl number
$Re$	Reynolds number
$t$	Time (s)
$T$	Temperature (K)
$U$	Horizontal velocity ( $\text{m}\cdot\text{s}^{-1}$ )
$V$	Vertical velocity ( $\text{m}\cdot\text{s}^{-1}$ )
$x$	Mole fraction
$X$	Horizontal length (m)
$Y$	Vertical length (m)

**Greek Symbols**

$\mu$	Dynamic viscosity ( $\text{kg}\cdot\text{m}^{-1}\text{s}^{-1}$ )
$\phi$	Volume concentration
$\rho$	Density ( $\text{kg}\cdot\text{m}^{-3}$ )
$\Theta$	Dimensionless temperature

**Subscripts**

avg	Average
C	Cold
f	Fluid (either PW or IL or PW + IL mixture or NEIL)
H	Hot
PW	Pure water

**Superscripts**

*	Dimensionless quantity
---	------------------------

**Abbreviations**

2D	Two-dimensional
CFD	Computational fluid dynamics
IL	Ionic liquid
NEIL	Nanoparticle enhanced ionic liquid
PW	Pure water

## 1 Introduction

Extraction of unwanted heat to maintain various electronic devices such as computer processors, bridge chips, integrated circuits within the operational limits is one of the challenging problems in the recent times [1]. However, from last two decades' numerous works have been carried out by changing different heat transfer fluids as well as by enhancing the thermal conductivity of the conventional fluids like pure water, methanol, ethylene glycol. [2]. One way of achieving high thermal conductivity fluids is by dispersing nanoparticles into the matrix of conventional heat transfer fluids thereby forming homogenous mixture called as "Nanofluids" [3]. Though these nanoparticle enhanced fluids called as "Nanofluids" are widely used in heat transfer research, still the mechanisms involved in enhancing the heat transfer were not completely understood and demonstrated. The choice of Nanofluids in regard to energy saving is not fully demonstrated as the increment in the viscosity causes an increase of pressure drop [4, 5].

On the other hand, usage of ionic liquids (ILs) is growing in the recent years due to the serious necessity in development of "green solvents" [6]. ILs are salts that possess low melting point (below 100 °C) [7]. The thermophysical properties and behavior of ILs used as heat transfer fluids will have considerable variation in comparison to molecular liquids and the low saturated vapor pressure at ambient condition is one of the important characteristics of ILs [8]. Though different heat efficient fluids are used in cooling applications, the one very important considerable disadvantage especially in electronic cooling is the leakage of liquid coolant that may cause severe damage to the entire device. To avoid this problem, usage of closed system rather than open system is preferable. In closed system, the heat transfer fluid will not cross the boundary of the control volume. Nimmagadda et al. [9, 10] conducted studies on closed cavity in which heat transfer fluid is driven by means of a moving lid. The studies also used various types of nanoparticles enhanced liquids and their associated heat transfer performance is evaluated.

Minea [11] presented an overview of ILs towards heat transfer performance. The overview showed that ILs can be an alternative to conventional heat transfer fluids and crucial attention was made towards analyzing their heat transfer coefficient. Wadekar [8] practically assessed the use of 1-butyl-3-methylimidazolium Bismide IL in heat transfer performance of shell and tube heat exchanger as well as in plate heat exchanger. The observation concluded that reasonable heat transfer coefficients can be obtained using suitable heat transfer enhancement technology with ILs. Ionano fluids (NEILs) obtained by multiwalled carbon nanotubes are studied by Franca et al. [12] to evaluate the thermal conductivity. The study showed that dispersing nanoparticles in ionic liquids increases the heat transfer area. Chernikova et al. [13] concluded that low saturated vapor pressure of ILs at high temperature makes them as non-explosive as well as non-volatile. They are more attractively used in dynamic vacuum operations and outer space. Zhang et al. [14] dispersed Graphene Nano platelets in ILs. The study concluded that by dispersing Nanoplatelets, the thermal conductivity of NEILs is increased by 43.2 % at 373.15 K near a mass fraction of 5 %.

A review on Nanofluids with ILs was presented by Minea and Murshed [15]. The review shows that ILs were implemented in CFD for analyzing their behavior in various thermal systems. Larger uncertainty is also present in evaluating the thermophysical properties of these ionano fluids. Thermophysical properties of NEILS are experimentally studied by Paul et al. [16] using  $\text{Al}_2\text{O}_3$  nanoparticles. The study showed that NEILS exhibited enhancement in thermal conductivity, heat capacity and viscosity when compared with pure ILs. Extensive multiscale studies are carried out by Dong et al. [17] which concludes the potential use of ILs in relevance to green technologies and optimizing the design with processing control of new materials is essential for industrialization of ILs. Chen et al. [18] observed that SiC ionano fluids have increased thermal conductivity which makes them suitable as efficient heat transfer fluid.

The potential of NEILs as advanced heat transfer fluid is presented by Bridges et al. [19]. The observations concluded that  $\text{Al}_2\text{O}_3$  nanoparticle based NEILs exhibits 30 % increment in heat capacity. The improvement in thermal stability of NEILs without any volatilization makes it appropriate as advanced heat transfer fluid.  $\text{Al}_2\text{O}_3$  nanoparticles based ILs exhibited 6 % increment in thermal conductivity, 23 % increment in heat capacity and 20 % increment in convective heat transfer performance for 1 weight% [20]. Liu et al. [21] also concluded that thermodynamic properties of Graphene based ionano fluids are superior where compared to commercial heat transfer fluid. Ribeiro et al. [22] concluded that increased heat storage capacity of ionano fluids where compared to traditional heat transfer fluids are responsible for their potential usage in heat exchangers. Tiznobaik and Shin [23] suggested that quantitative analysis is necessary for nanostructure thermal characteristics as well as for investigating the inadaptability of nanoparticles dispersion in ILs.

However, as mentioned in the above stated literature, use of closed system especially in the application of cooling of electronic devices is very advantageous [9, 10]. Moreover, it is adaptable to use ILs as an alternative to conventional heat transfer fluids [11, 15, 22] and they fall into the category of green solvents [6, 13]. Furthermore, dispersing nanoparticles into the matrix of IL will form NEILS also called as ionano fluids with enhanced thermal conductivity [12, 14, 18]. Bringing together all these individual key characteristics into one common study and obtaining the heat transfer performance of Pure water,  $[\text{C}_2\text{mim}][\text{CH}_3\text{SO}_3]$  ionic liquid, ionic liquid mixtures (PW + IL) and  $\text{Al}_2\text{O}_3$  nanoparticle enhanced ionic liquids is the motivation for present investigation. Also, among three different types of lid-driven cavities such as normal, uni-directional and bi-directional; which lid-driven cavity type will give better heat transfer performance is also investigated in the present study. It is also to be understood that to make the obtained results to be reliable, the used 2D in-house code based on single phase approach is primarily validated against the experimental and numerical results available in the literature.

## 2 Geometry Description

The 2D geometry description adopted in the present investigation is shown in Fig. 1. Three cases are considered, and in all of them, the cavity remains square with length (L) and height (h) as 0.001 m. In Case-1, as shown in Fig. 1a, the top lid will be

moving in the direction of positive  $X$ -axis forming it as a normal lid-driven cavity problem. Whereas in Case-2 and Case-3, as shown in Fig. 1b and c, two moving lids are present on top and bottom of the cavity. In Case-2, the two lids will move in same direction that is in the direction of positive  $X$ -axis there by forming it as uni-directional lid-driven cavity problem. Moreover, in Case-3, the two lids will move in opposite direction (top lid will move in the direction of positive  $X$ -axis and the bottom lid will move in the direction of negative  $X$ -axis) there by forming it as bi-directional lid-driven cavity problem. The heat transfer fluid that is present within the square cavity in all the three cases will be driven by means of moving lids and the associated heat transfer performance is assessed for steady state laminar flow ( $Re = 1100$  to  $1900$ ) of various fluids such as pure water,  $[C_2mim][CH_3SO_3]$  ionic liquid, ionic liquid mixtures (PW + IL) and  $Al_2O_3$  nanoparticle enhanced ionic liquids.

### 3 Thermophysical Properties

The thermophysical properties of all the heat transfer fluids used in the present investigation were experimentally measured by Chereches et al. [24, 25]. Table 1 represents the thermophysical properties of pure water (PW),  $[C_2mim][CH_3SO_3]$  ionic liquid (IL), ionic liquid mixtures (PW + IL) and  $Al_2O_3$  nanoparticle enhanced ionic liquids (NEILS) at room temperature. In the case of ionic liquid mixtures, naming is given using the format  $x_{PW}PW + (1 - x_{PW})IL$  in which  $x_{PW}$  represents the mole fraction of pure water. Thus, as shown in Table 1,  $0.25PW + 0.75IL$  mixture contains mole fraction of pure water as 0.25. As reported in Chereches et al. [24], the average size of dispersed  $Al_2O_3$  nanoparticles used in this study is 50 nm. Moreover, the IL is also soluble in water.

### 4 Mathematical Formulation

Two-dimensional numerical investigation has been carried out using an in-house CFD code for studying steady state laminar flow of PW, IL, PW + IL mixtures, and  $Al_2O_3$  NEILS within a lid-driven cavity problem. The CFD code was programmed in C++

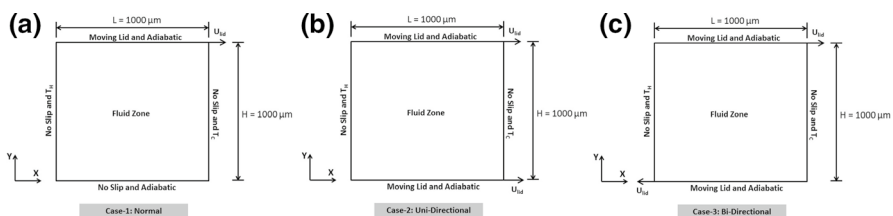


**Fig. 1** Geometry description: (a) Case-1: normal cavity with top lid moving, (b) Case-2: uni-directional cavity with top and bottom lids moving in same direction, and (c) Case-3: bi-directional cavity with top and bottom lids moving in opposite directions

**Table 1** Thermophysical properties of pure water, ionic liquids and NEILS as per Chereches et al. [24, 25]

S. no.	Heat transfer fluid	Density ( $\text{kg}\cdot\text{m}^{-3}$ )	Thermal conductivity ( $\text{W}\cdot\text{m}^{-1}\text{K}^{-1}$ )	Dynamic viscosity ( $\text{kg}\cdot\text{m}^{-1}\text{s}^{-1}$ )	Specific heat ( $\text{J}\cdot\text{kg}^{-1}\text{K}^{-1}$ )	Nanoparticle volume concentration
1	PW	997.8	0.598	0.001	4182	0
2	IL	1242.6	0.188	0.154	1696.9	0
3	0.25PW + 0.75IL	1237	0.201	0.0533	1771.9	0
4	0.50PW + 0.50IL	1224.9	0.201	0.0143	1855.2	0
5	0.75PW + 0.25IL	1193.8	0.229	0.0038	2195	0
6	1 % wt. in 0.25PW + 0.75IL	1243.8	0.195	0.0803	1817.7	0.0032
7	2.5 % wt. in 0.25PW + 0.75IL	1257.3	0.197	0.0831	1807	0.008
8	5 % wt. in 0.25PW + 0.75IL	1275.4	0.201	0.108	1795.1	0.016
9	10 % wt. in 0.25PW + 0.75IL	1314.5	0.21	0.133	1771.3	0.0339
10	15 % wt. in 0.25PW + 0.75IL	1353.2	0.222	0.205	1751.6	0.0527

and is based on finite volume method. The governing equations, boundary conditions and evaluation of Nusselt number is given in the below subsections.

### 4.1 Governing Equations

The heat transfer fluid that is present within the cavity is incompressible and the fluid motion due to the driving lid falls under laminar regime. The governing equations for this 2D laminar incompressible motion of fluid are mathematically given by Navier–Stokes equations. The continuity, momentum and energy equations are represented in dimensionless form using different scaling factors as shown in Table 2.

The final non-dimensional equations for both the velocity as well as temperature fields are as follows:

$$\frac{\partial U^*}{\partial X^*} + \frac{\partial V^*}{\partial Y^*} = 0 \tag{1}$$

$$\frac{\partial U^*}{\partial t^*} + U^* \frac{\partial U^*}{\partial X^*} + V^* \frac{\partial U^*}{\partial Y^*} = -\frac{\partial p^*}{\partial X^*} + \frac{1}{\text{Re}} \left( \frac{\partial^2 U^*}{\partial X^{*2}} + \frac{\partial^2 U^*}{\partial Y^{*2}} \right) \tag{2}$$

$$\frac{\partial V^*}{\partial t^*} + U^* \frac{\partial V^*}{\partial X^*} + V^* \frac{\partial V^*}{\partial Y^*} = -\frac{\partial p^*}{\partial Y^*} + \frac{1}{\text{Re}} \left( \frac{\partial^2 V^*}{\partial X^{*2}} + \frac{\partial^2 V^*}{\partial Y^{*2}} \right) \tag{3}$$

$$\frac{\partial \theta}{\partial t^*} + U^* \frac{\partial \theta}{\partial X^*} + V^* \frac{\partial \theta}{\partial Y^*} = \frac{1}{\text{Re Pr}} \left( \frac{\partial^2 \theta}{\partial X^{*2}} + \frac{\partial^2 \theta}{\partial Y^{*2}} \right) \tag{4}$$

The dimensionless numbers Re and Pr mentioned in the above equations are given as:  $\text{Re} = \frac{\rho_f \cdot U_{\text{lid}} \cdot L}{\mu_f}$ ,  $\text{Pr} = \frac{\mu_f \cdot C_{p_f}}{k_f}$  respectively.

### 4.2 Boundary Conditions

All the four walls of the cavity are subjected to appropriate velocity and temperature boundary conditions to obtain reliable results. No slip velocity boundary condition ( $U^*=0$  and  $V^*=0$ ) is implemented on all the stationary walls of the cavity. For the walls moving in the direction of positive X-axis, the velocity boundary condition represented by  $U^*=1$  and  $V^*=0$  is implemented. However, if the wall is moving in negative X-axis direction, then  $U^*=-1$  and  $V^*=0$  boundary condition is implemented. The values of Reynolds number used in the present investigation lie in the range of 1100 to 1900. Both the bottom and top horizontal walls are insulated thereby they are subjected

**Table 2** Dimensionless scaling factors used in non-dimensionalizing the governing equations

Velocity	Length	Time	Temperature	Pressure
$U^* = \frac{U}{U_{\text{lid}}}, V^* = \frac{V}{U_{\text{lid}}}$	$X^* = \frac{X}{L}, Y^* = \frac{Y}{L}$	$t^* = \frac{t}{L-U_{\text{lid}}}$	$\theta = \frac{T-T_c}{T_H-T_c}$	$P^* = \frac{p}{\rho_f U_{\text{lid}}^2}$

to a temperature boundary condition of  $\frac{\partial \theta}{\partial Y^*} = 0$ . The left vertical wall of the cavity is subjected to hot temperature ( $T_H$ ) giving rise to  $\theta = 1$ . Whereas, the right vertical wall of the cavity is subjected to cold temperature ( $T_C$ ) giving rise to  $\theta = 0$ .  $T_H$  and  $T_C$  values are not presented exclusively as the representation of obtained variables is completely done in dimensionless form.

### 4.3 Nusselt Number Evaluation

The local Nusselt number ( $Nu_{local}$ ) is evaluated mathematically as given below along the left vertical wall of the cavity to which  $T_H$  is applied and by integrating this  $Nu_{local}$  value will result in average Nusselt number ( $Nu_{avg}$ ).

$$Nu_{local} = \frac{hL}{k_{PW}} = \frac{-k_f}{k_{PW}} \left( \frac{\partial \theta}{\partial X^*} \right) \quad (5)$$

## 5 Numerical method

The set of governing equations as given in Sect. 4.1 are initially discretized using finite volume method. These discretized equations are then solved on collocated grid [26] with the use of simplified marker and cell (SMAC) algorithm. The algorithm is also equipped with Rhie-Chow momentum interpolation technique for avoiding the decoupling nature of pressure–velocity on non-staggered grid [27]. Both upwind and central difference schemes were used for the discretization of convection and diffusion terms, respectively. Small time steps are used with explicit first-order Euler time integration to avoid numerical instability and forward marching of the solution was carried out with time integration.

## 6 Validation

The developed 2D in-house CFD code is validated against the results of well-known Shah and London correlation [28] as well as with Liu et al. [29], and Manay and Sahin [30] experimental results. In order to obtain this relative comparison, the geometrical dimensions as well as the boundary conditions given in Manay and Sahin [30] are implemented in the present 2D in-house CFD code. The  $Nu_{avg}$  values at different Re for pure water in a micro-channel are used for this validation. Figure 2 shows the comparison of  $Nu_{avg}$  values obtained by present model with the available results in the literature at different Re. From Fig. 2, it is clearly understood that the developed 2D in-house CFD code shows a good match with the experimental  $Nu_{avg}$  values available in the literature.



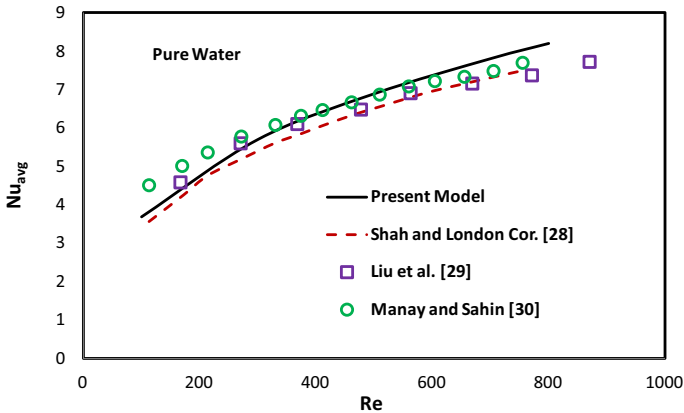


**Fig. 2** Comparison of  $Nu_{avg}$  values obtained by present model with the available results in the literature for pure water in a micro-channel at different  $Re$

## 7 Grid Dependency

Grid dependency study was conducted to obtain the optimum grid size beyond which the accuracy in the obtained results will not change. This will help in getting reliable results by having a balance between computational time and computational cost. Three different types of lid-driven cavities such as normal, uni-directional and bi-directional represented as Case-1, Case-2 and Case-3 as shown in Fig. 1 are chosen for carrying out grid dependency study. The average Nusselt number values of pure water at  $Re=1900$  for different grid sizes are given in Table 3. From Table 3, it can be clearly seen that the  $Nu_{avg}$  values obtained for  $150 \times 150$  grid size in all the three cases has very small incremental variation of 1.57 %, 1.68 % and 1.67 % respectively in comparison with the value obtained for  $200 \times 200$  grid size. In this regard,  $150 \times 150$  grid size is selected as optimum grid size in the present investigation.

## 8 Results and Discussion

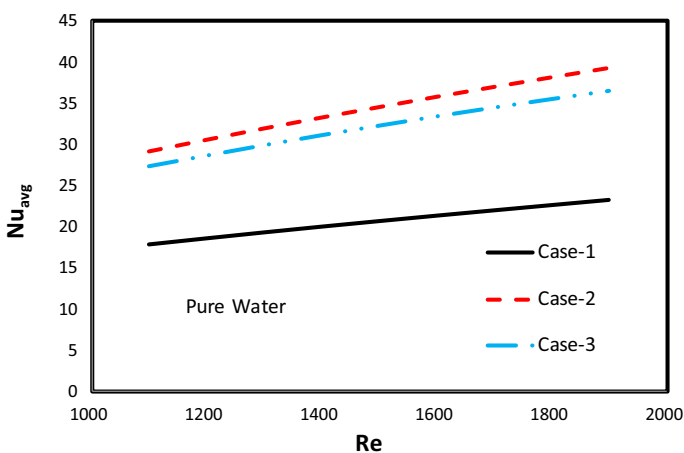
Two-dimensional numerical investigation has been carried out using an in-house CFD code for studying steady state laminar flow of pure water,  $[C_2mim]$   $[CH_3SO_3]$  ionic liquid, ionic liquid mixtures (PW + IL) and  $Al_2O_3$  nanoparticle enhanced ionic liquids within a lid-driven cavity problem. The associated heat transfer performance is assessed for  $Re=1100$  to  $1900$  for all the above fluids in all the three cases represented as normal, uni-directional and bi-directional lid-driven cavities. The following results are obtained from this numerical investigation.

**Table 3**  $Nu_{avg}$  values of pure water at  $Re = 1900$  for different grid sizes in all the three types of lid-driven cavities

Grid size	$Nu_{avg}$ of pure water		
	Case-1 (Normal)	Case-2 (Uni-directional)	Case-3 (Bi-directional)
$50 \times 50$	23.0447	35.6247	32.6822
$100 \times 100$	23.6200	39.6587	36.8065
$125 \times 125$	23.4381	39.5397	36.7292
$150 \times 150$ (selected grid)	23.2413	39.2260	36.4783
$175 \times 175$	23.0535	38.8909	36.1791
$200 \times 200$	22.8829	38.5771	35.8776

### 8.1 Effect of Lid-Driven Cavity Type

The effect of lid-driven cavity type on the average Nusselt number values of pure water at different  $Re$  is shown in Fig. 3 for normal (Case-1), uni-directional (Case-2) and bi-directional (Case-3) lid-driven cavities. From Fig. 3, it is clearly seen that Case-2 and Case-3 exhibits higher heat transfer performance in comparison with Case-1. This is due to the presence of only one moving lid in Case-1. Whereas, in other two cases, two moving lids are present that are responsible for driving the heat transfer fluid. Due to this, forced convection phenomenon is dominant in Case-2 and Case-3 when compared with Case-1. Furthermore, Case-2 exhibits higher heat transfer performance in comparison with Case-3. This is caused due to the reason that in uni-directional lid-driven cavity, the two horizontal lids move with same velocity in same direction that too away from the high temperature wall. This causes

**Fig. 3**  $Nu_{avg}$  values at different  $Re$  of pure water in normal (Case-1), uni-directional (Case-2) and bi-directional (Case-3) lid-driven cavities

the fluid within the cavity to drive faster over the high temperature wall and forms two circular zones one above the other as observed in the streamline contours of Fig. 4b. Moreover, these two circular fluid zones swirl in opposite direction with top zone swirling in clockwise and bottom zone swirling in anticlockwise directions. The obtained results showed that uni-directional lid-driven cavity exhibits 68.78 % higher  $Nu_{avg}$  value at  $Re=1900$  in comparison with normal lid-driven cavity for pure water. Whereas, as seen in Fig. 4a and c, Case-1 and Case-3 has only one swirling fluid zone with faster fluid drive in Case-3 as a result of the presence of two moving lids.

## 8.2 Velocity and Temperature Contours

The velocity and temperature contours of pure water,  $[C_2mim][CH_3SO_3]$  ionic liquid and 15 % wt  $Al_2O_3$  nanoparticles enhanced ionic liquid in uni-directional lid-driven cavity are shown in Fig. 5. From Fig. 5a, it is understood that the velocity contours represented by solid line, dotted line and dashed line for pure water, ionic liquid and NEIL overlap with each other. This is due to the non-dimensionalization of velocity field of respective heat transfer fluid with corresponding lid velocity obtained for that particular fluid. However, in Fig. 5b, the temperature field of pure water, ionic liquid and NEIL shows some deviation. This is caused due to the difference in the thermal conductivities of all these three fluids.

## 8.3 Effect of Different Heat Transfer Fluids

The effect of different heat transfer fluids on the average Nusselt number values in uni-directional lid-driven cavity at different  $Re$  is shown in Fig. 6. Pure water,  $[C_2mim][CH_3SO_3]$  ionic liquid and three different mixtures (0.25PW + 0.75IL, 0.5PW + 0.5IL, 0.75PW + 0.25IL) are used in this comparison. From Fig. 6, it is understood that  $[C_2mim][CH_3SO_3]$  ionic liquid exhibits higher heat transfer performance in comparison with other heat transfer fluids. At  $Re=1900$ , 115.48 % higher  $Nu_{avg}$  value is obtained for  $[C_2mim][CH_3SO_3]$  ionic liquid in comparison with pure water. This is due to its significant higher value of lid velocity when compared

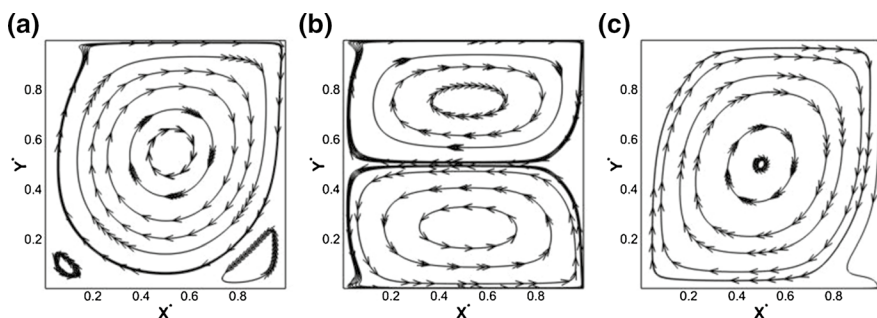


**Fig. 4** Streamlines of pure water at  $Re=1900$  in (a) normal (Case-1), (b) uni-directional (Case-2), and (c) bi-directional (Case-3) lid-driven cavities

**Fig. 5** Contours of pure water (solid line), ionic liquid (dotted line) and 15 % wt NEIL (dashed line) at  $Re = 1900$  in Case-2: (a) velocity, and (b) temperature

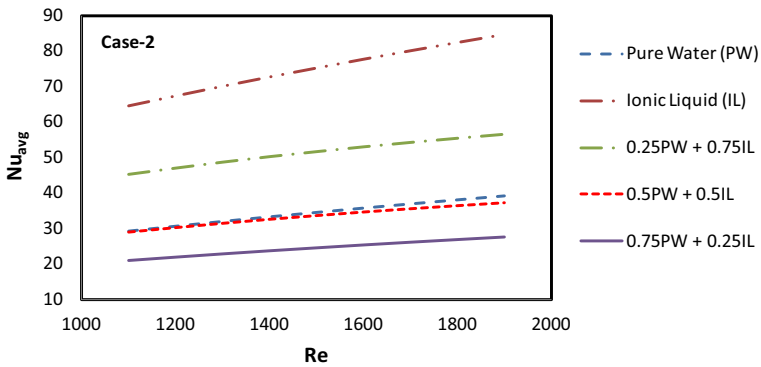
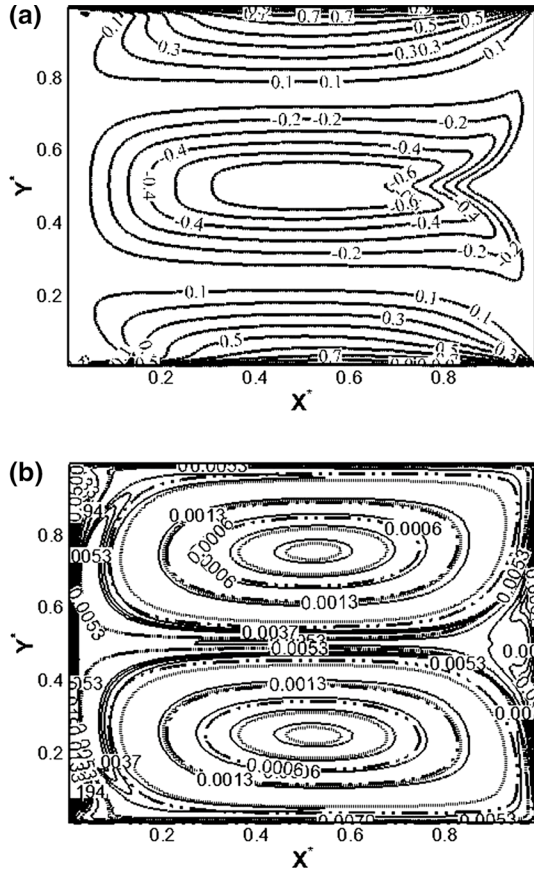


**Fig. 6** Average Nusselt number values of different heat transfer fluids at different Reynolds number in uni-directional lid-driven cavity

with pure water. The lid velocity values obtained for pure water and ionic liquid at  $Re=1900$  are found to be  $1.9042 \text{ m}\cdot\text{s}^{-1}$  and  $235.474 \text{ m}\cdot\text{s}^{-1}$ , respectively. The lid velocities of different heat transfer fluids used in the present study are given in Table 4 for different  $Re$ . The significant higher lid velocity values in the case of ionic liquid are due to its high viscosity value when compared with other heat transfer fluids. Even though the density of ionic liquid is slightly higher than that of pure water, the significant increment in its dynamic viscosity value when compared with that of pure water is responsible for higher lid velocity in the case of ionic liquid at any given  $Re$ . For mixtures of pure water and ionic liquid, the viscosity value gradually decreases with increase in the proportion of pure water. This results in the decrement of lid velocity for pure water and ionic liquid mixtures with increment in the proportion of pure water in it. Moreover, from Fig. 6, it is also understood that  $0.75PW + 0.25IL$  mixture shows lower  $Nu_{avg}$  values in comparison with pure water even though its lid velocity is higher than pure water. This is due to the significant lower thermal conductivity value of  $0.75PW + 0.25IL$  mixture when compared to the increment in the lid velocity with respect to pure water. Furthermore, it is also observed from Fig. 6 that  $0.5PW + 0.5IL$  mixture shows almost similar  $Nu_{avg}$  values in comparison with pure water even though its lid velocity is higher than pure water. This is caused due to the higher lid velocity in the case of  $0.5PW + 0.5IL$  mixture is balanced by its lower thermal conductivity value in comparison with pure water and as a result they both exhibit almost similar heat transfer performance. The heat transfer performance of Pure water, ionic liquid and three different mixtures at different  $Re$  are also represented in dimensional form as shown in Table 5 in terms of average convective heat transfer coefficient.

#### 8.4 Effect of Nanoparticle Enhanced Ionic Liquids

The effect of different concentrations of  $Al_2O_3$  nanoparticles dispersed in  $0.25PW + 0.75IL$  mixture on the average Nusselt number values in uni-directional lid-driven cavity at different  $Re$  is shown in Fig. 7. Pure water,  $[C_2mim][CH_3SO_3]$  ionic liquid and 1 % wt, 5 % wt, 15 % wt  $Al_2O_3$  nanoparticles dispersed in  $0.25PW + 0.75IL$  mixture (NEILS) are used in this comparison. From Fig. 7, it is understood that 15 % wt NEIL exhibits higher heat transfer performance when compared to other heat transfer fluids. At  $Re = 1900$ , 161.16 % higher  $Nu_{avg}$

**Table 4** Lid velocities of different heat transfer fluids at different  $Re$

Re	$U_{lid} \text{ (m}\cdot\text{s}^{-1}\text{)}$				
	Pure water	Ionic liquid	0.25PW + 0.75IL	0.50PW + 0.50IL	0.75PW + 0.25IL
1100	1.1024	136.3271	47.3969	12.8419	3.5014
1300	1.3029	161.1138	56.0146	15.1767	4.1380
1500	1.5033	185.9005	64.6322	17.5116	4.7747
1700	1.7037	210.6873	73.2498	19.8465	5.4113
1900	1.9042	235.4740	81.8674	22.1814	6.0479

**Table 5** Average convective heat transfer coefficient of different heat transfer fluids at different Re

Re	$h_{avg}$ ( $W \cdot m^{-2} K^{-1}$ )				
	Pure water	Ionic liquid	0.25PW + 0.75IL	0.50PW + 0.50IL	0.75PW + 0.25IL
1100	17394.38	38647.35	27016.81	17269.40	12448.19
1300	19060.47	41908.58	29102.39	18776.05	13592.32
1500	20611.62	44944.78	30896.31	20102.01	14641.99
1700	22078.28	47821.37	32472.56	21274.85	15620.53
1900	23457.15	50544.55	33871.52	22304.97	16525.42

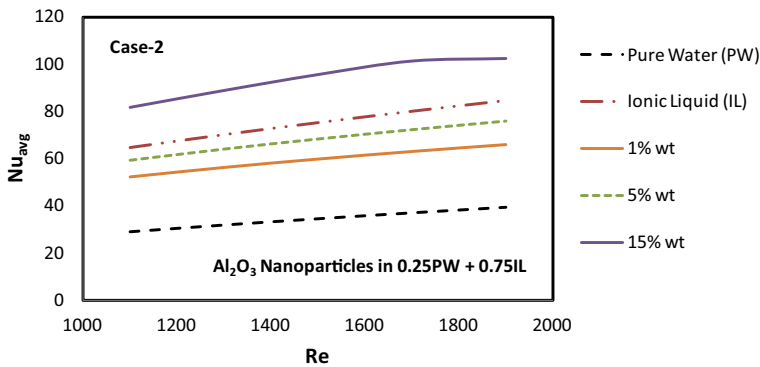


**Fig. 7** Average Nusselt number values of nanoparticle enhanced ionic liquids at different Reynolds number in uni-directional lid-driven cavity

**Table 6** Lid velocities of different concentrations of nanoparticle enhanced ionic liquids at different Re

Re	$U_{lid}$ ( $m \cdot s^{-1}$ )				
	Pure water	Ionic liquid	0.25PW + 0.75IL		
			1 % wt $Al_2O_3$	5 % wt $Al_2O_3$	15 % wt $Al_2O_3$
1100	1.1024	136.3271	71.0162	93.1472	166.6420
1300	1.3029	161.1138	83.9283	110.0831	196.9406
1500	1.5033	185.9005	96.8403	127.0190	227.2391
1700	1.7037	210.6873	109.7524	143.9548	257.5377
1900	1.9042	235.4740	122.6644	160.8907	287.8362

value is obtained for 15 % wt NEIL in comparison with pure water. This is due to its significant higher value of lid velocity when compared with pure water. The lid velocity values obtained for pure water and 15 % wt NEIL at  $Re = 1900$  are found to be  $1.9042 \text{ m}\cdot\text{s}^{-1}$  and  $287.8362 \text{ m}\cdot\text{s}^{-1}$ , respectively. The lid velocities of different concentrations of NEILs at different  $Re$  used in the present study are given in Table 6 for different  $Re$ . The significant higher lid velocity values in the case of 15 % wt NEIL are due to its high viscosity value when compared with other heat transfer fluids. An increment of 33.12 % and 8.9 % is obtained for dynamic viscosity and density values respectively in the case of 15 % wt NEIL when compared with ionic liquid. For any given  $Re$ , this significant increment in the dynamic viscosity is responsible for higher lid velocity in the case of 15 % wt NEIL when compared with ionic liquid. For 1 % wt and 5 % wt NEILs, the viscosity values are lower than that of ionic liquid. This results in the decrement of lid velocity as shown in Table 6 for 1 % wt and 5 % wt NEILs which in turn is responsible for their lower  $Nu_{avg}$  values when compared with ionic liquid as observed in Fig. 7. The heat transfer performance of Pure water, ionic liquid and 1 % wt, 5 % wt, 15 % wt  $Al_2O_3$  NEILs at different  $Re$  are also represented in dimensional form as shown in Table 7 in terms of average convective heat transfer coefficient.

**Table 7** Average convective heat transfer coefficient of different concentrations of nanoparticle enhanced ionic liquids at different  $Re$

Re	$h_{avg}$ ( $W\cdot m^{-2} K^{-1}$ )				
	Pure water	Ionic liquid	0.25PW + 0.75IL		
			1 % wt $Al_2O_3$	5 % wt $Al_2O_3$	15 % wt $Al_2O_3$
1100	17394.38	38647.35	31125.32	35426.65	48882.40
1300	19060.47	41908.58	33526.55	38225.98	53160.56
1500	20611.62	44944.78	35652.63	40756.17	57188.31
1700	22078.28	47821.37	37578.26	43092.19	60611.55
1900	23457.15	50544.55	39332.28	45255.15	61260.23

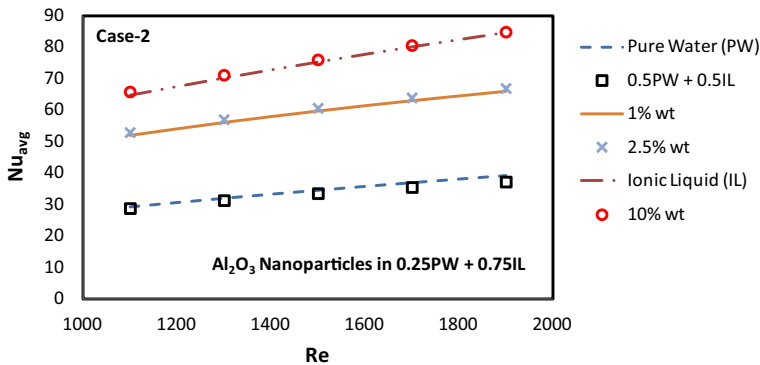


**Fig. 8** Average Nusselt number values of fluids exhibiting equivalent heat transfer performance at different Reynolds number in uni-directional lid-driven cavity

### 8.5 Equivalent Heat Transfer Fluids

Average Nusselt number values of fluids exhibiting equivalent heat transfer performance at different Reynolds number in uni-directional lid-driven cavity are shown in Fig. 8. Three equivalent heat transfer fluid pairs: pure water and 0.5PW + 0.5IL, 1 % wt and 2.5 % wt NEILs, 10 % wt NEIL and  $[C_2mim][CH_3SO_3]$  ionic liquid are observed in the present investigation based on their similar heat transfer performance. As explained in Fig. 6, 0.5PW + 0.5IL mixture shows almost similar  $Nu_{avg}$  values in comparison with pure water even though its lid velocity is higher than pure water. This is caused due to the higher lid velocity in the case of 0.5PW + 0.5IL mixture is balanced by its lower thermal conductivity value in comparison with pure water and as a result they both exhibit almost similar heat transfer performance. Moreover, as observed in Table 1, at lower concentrations of dispersed  $Al_2O_3$  nanoparticles in ionic liquid, the thermal conductivity and dynamic viscosity values do not vary much when compared with each other. This is the reason; both 1 % wt and 2.5 % wt NEILs exhibit almost similar heat transfer performance as observed in Fig. 8 forming an equivalent heat transfer fluid pair. Furthermore, 10 % wt NEIL and  $[C_2mim][CH_3SO_3]$  ionic liquid has almost similar thermal conductivity values and dynamic viscosity values. Even in these similar values, 10 % wt NEIL has higher thermal conductivity and lower viscosity when compared with  $[C_2mim][CH_3SO_3]$  ionic liquid as observed in Table 1. As a result of this, the lower lid velocity value in the case of 10 % wt NEIL is balanced by its high thermal conductivity value and hence 10 % wt NEIL exhibits similar  $Nu_{avg}$  values in comparison with ionic liquid as observed in Fig. 8 forming an equivalent heat transfer fluid pair.



## 9 Conclusion

Two-dimensional numerical investigation has been carried out using an in-house CFD code for studying steady state laminar flow of pure water,  $[C_2mim][CH_3SO_3]$  ionic liquid, ionic liquid mixtures (PW + IL) and  $Al_2O_3$  nanoparticle enhanced ionic liquids within a lid-driven cavity problem. The associated heat transfer performance is assessed for  $Re = 1100$  to  $1900$  for all the above fluids in all the three cases represented as normal, uni-directional and bi-directional lid-driven cavities. The following conclusions are obtained from this numerical investigation.

- The presence of two moving lids in the case of uni-directional lid-driven cavity is responsible for its 68.78 % higher  $Nu_{avg}$  value in comparison with normal lid-driven cavity for pure water at  $Re = 1900$ .
- Significant higher lid velocity in the case of  $[C_2mim][CH_3SO_3]$  ionic liquid leads to 115.48 % higher  $Nu_{avg}$  value when compared with pure water at  $Re = 1900$ .
- Significant higher lid velocity values in the case of 15 % wt  $Al_2O_3$  nanoparticles in 0.25PW + 0.75IL gives rise to 21.2 % and 161.16 % higher heat transfer performance when compared with ionic liquid and pure water at  $Re = 1900$ .
- For any given  $Re$ , the higher lid velocity values are due to significant increment in the dynamic viscosity. An increment of 33.12 % and 8.9 % is obtained for dynamic viscosity and density values respectively in the case of 15 % wt NEIL when compared with ionic liquid.
- Three equivalent heat transfer fluid pairs: pure water and 0.5PW + 0.5IL, 1 % wt and 2.5 % wt NEILs, 10 % wt NEIL and  $[C_2mim][CH_3SO_3]$  ionic liquid are observed in which each pair exhibits similar heat transfer performance.

**Funding** There are no funding sources associated with this work.

**Declarations**

**Conflict of interest** The authors declare that they do not have any type of conflict.

## References

1. S.S. Murshed, *Electronics Cooling* (IntechOpen, London, 2016), p. 1. <https://doi.org/10.5772/63321>
2. E.C. Okonkwo, I. Wole-Osho, I.W. Almanassra, Y.M. Abdullatif, T. Al-Ansari, J. Therm. Anal. Calorim. (2020). <https://doi.org/10.1007/s10973-020-09760-2>
3. S.U. Choi, J.A. Eastman, *Enhancing Thermal Conductivity of Fluids with Nanoparticles* (No. ANL/MSD/CP-84938; CONF-951135-29) (Argonne National Lab, Lemont, 1995).
4. S. Malekian, E. Fathi, N. Malekian, H. Moghadasi, M. Moghimi, Int. J. Thermophys. **39**, 100 (2018). <https://doi.org/10.1007/s10765-018-2422-z>
5. C. Li, Z. Zhao, X. Zhang, T. Li, Int. J. Thermophys. **39**, 41 (2018). <https://doi.org/10.1007/s10765-018-2359-2>

6. H. Zhao, Chem. Eng. Commun. **193**, 1660–1677 (2006). <https://doi.org/10.1080/00986440600586537>
7. F.U. Shah, R. An, N. Muhammad, Front. Chem. (2020). <https://doi.org/10.3389/fchem.2020.627213>
8. V.V. Wadekar, Appl. Therm. Eng. **111**, 1581–1587 (2017). <https://doi.org/10.1016/j.applthermaleng.2016.04.156>
9. R. Nimmagadda, R. Reuven, L.G. Asirvatham, S. Wongwises, IEEE Trans. Compon. Packag. Manuf. Technol. **10**, 1868–1878 (2020). <https://doi.org/10.1109/TCPMT.2020.3008786>
10. R. Nimmagadda, D.P. Matta, R. Reuven, L.G. Asirvatham, S. Wongwises, A. Yerramilli, S. Adu-sumilli, *ASME Power Conference*, vol. 83747 (American Society of Mechanical, New York, 2020), p. V001T11A004. <https://doi.org/10.1115/POWER2020-16696>
11. A.A. Minea, Int. J. Thermophys. **41**, 1–15 (2020). <https://doi.org/10.1007/s10765-020-02727-3>
12. J.M. França, M.J.V. Lourenço, S.S. Murshed, A.A. Pádua, C.A. Nieto de Castro, Ind. Eng. Chem. Res. **57**, 6516–6529 (2018). <https://doi.org/10.1021/acs.iecr.7b04770>
13. E.A. Chernikova, L.M. Glukhov, V.G. Krasovskiy, L.M. Kustov, M.G. Vorobyeva, A.A.E. Koroteev, Russ. Chem. Rev. **84**, 875 (2015). <https://doi.org/10.1070/RCR4510>
14. F.F. Zhang, F.F. Zheng, X.H. Wu, Y.L. Yin, G. Chen, R. Soc. Open Sci. **6**, 182040 (2019). <https://doi.org/10.1098/rsos.182040>
15. A.A. Minea, S.S. Murshed, Renew. Sustain. Energy Rev. **91**, 584–599 (2018). <https://doi.org/10.1016/j.rser.2018.04.021>
16. T.C. Paul, A.K.M.M. Morshed, E.B. Fox, J.A. Khan, Appl. Therm. Eng. **110**, 1–9 (2017). <https://doi.org/10.1016/j.applthermaleng.2016.08.004>
17. K. Dong, X. Liu, H. Dong, X. Zhang, S. Zhang, Chem. Rev. **117**, 6636–6695 (2017). <https://doi.org/10.1021/acs.chemrev.6b00776>
18. W. Chen, C. Zou, X. Li, Sol. Energy Mater. Sol. Cells **163**, 157–163 (2017). <https://doi.org/10.1016/j.solmat.2017.01.029>
19. N.J. Bridges, A.E. Visser, E.B. Fox, Energy Fuels **25**, 4862–4864 (2011). <https://doi.org/10.1021/ef2012084>
20. T.C. Paul, A.M. Morshed, J.A. Khan, Procedia Eng. **56**, 631–636 (2013). <https://doi.org/10.1016/j.proeng.2013.03.170>
21. J. Liu, F. Wang, L. Zhang, X. Fang, Z. Zhang, Renew. Energy **63**, 519–523 (2014). <https://doi.org/10.1016/j.renene.2013.10.002>
22. A.P.C. Ribeiro, S.I.C. Vieira, J.M. França, C.S. Queirós, E. Langa, M.J.V. Lourenço, C.N. de Castro, *Ionic Liquids: Theory, Properties, New Approaches* (IntechOpen, London, 2011). <https://doi.org/10.5772/13920>
23. H. Tiznobaik, D. Shin, Appl. Phys. Lett. **102**, 173906 (2013). <https://doi.org/10.1063/1.4801645>
24. E.I. Cherecheş, J.I. Prado, M. Cherecheş, A.A. Minea, L. Lugo, J. Mol. Liq. **291**, 111332 (2019). <https://doi.org/10.1016/j.molliq.2019.111332>
25. E.I. Cherecheş, J.I. Prado, C. Ibanescu, M. Danu, A.A. Minea, L. Lugo, J. Mol. Liq. **317**, 114020 (2020). <https://doi.org/10.1016/j.molliq.2020.114020>
26. L. Cheng, S. Armfield, Int. J. Numer. Methods Fluids **21**, 15–34 (1995). <https://doi.org/10.1002/fld.1650210103>
27. C.M. Rhie, W.L. Chow, AIAA J. **21**, 1525–1532 (1983). <https://doi.org/10.2514/3.8284>
28. R.K. Shah, A.L. London, F.M. White, *Laminar Flow Forced Convection in Ducts* (Academic Press, New York, 1978).
29. C. Liu, J.T. Teng, J.C. Chu, Y.L. Chiu, S. Huang, S. Jin, T. Dang, R. Greif, H.H. Pan, Int. J. Heat Mass Transfer **54**, 3069–3080 (2011). <https://doi.org/10.1016/j.ijheatmasstransfer.2011.02.030>
30. E. Manay, B. Sahin, Heat Transfer Eng. **38**, 510–522 (2017). <https://doi.org/10.1080/10407782.2016.1195162>

**Publisher's Note** Springer Nature remains neutral with regard to jurisdictional claims in published maps and institutional affiliations.